Preprint Title Few-layer bismuthene for 1-μm ultrafast laser applications

Authors Tianci Feng, Xiaohui Li, Tong Chai, Penglai Guo, Ying Zhang, Ruisheng Liu, Jishu Liu, JiangBo Lu and Yanqi Ge

Article Type Full Research Paper

ORCID® iDs Xiaohui Li - https://orcid.org/0000-0002-5600-3820

Few-layer bismuthene for 1-μm ultrafast laser applications

Tianci Feng[1], Xiaohui Li[1], *, Tong Chai[1], Penglai Guo[1], Ying Zhang[1], Ruisheng Liu[1], Jishu Liu[1], JiangBo Lu[1], Yanqi Ge[3]

[1] School of Physics & Information Technology, Shaanxi Normal University, Xi'an 710119, China

[2] College of Electronic Science and Technology, Shenzhen University, Shenzhen, China.

* Author e-mail address: lixiaohui0523@163.com, geyanqi@hotmail.com.

Abstract

Bismuthene, as a new two-dimensional (2D) material made up of diazo metal elements, has drawn massive attention for its unique electronic, mechanical, and quantum properties. However, the nonlinear optical properties of bismuthene in 1-μm region, especially their applications for ultrafast photonics and internal ultrashort pulse dynamics, has seldom been explored yet. In this work, we investigate the few-layer bismuthene characterizations and apply it as a saturable absorber (SA) in a 1-μm ultrafast pulse generation. Thanks to the narrow bandgap of bismuthene and tapered fiber structure, A special noise like pulse has been obtained. The dynamics is also quite different from previous observed pulses, whose intensity ratio of coherent peak and envelope components is of around 5:4 from the autocorrelation trace. It's demonstrated that the abnormal noise-like pulses contain more uniform-intensity sub pulses. This proposed pulsed fiber laser based on bismuthene SA source is well suitable for some applications such as material processing, optical logics etc.

Keywords

bismuthene, abnormal noise-like pulse, evanescent field, ytterbium-doped fiber ring laser.

1. Introduction

In the past several years, bismuthene as a novel member of the 2D monatomic molecule material has attracted science researchers. As the heaviest element of group-VA, the two-dimensional (2D)-forms of β-bismuth crystal is characterized showing a semi-metallic property, while its single-layer structure is a narrow band gap semiconductor [1-5]. This new material must be some large-scale applications in industry along with the rapid progress in theoretical and experimental investigations.

As a desirable platform for the ultrafast pulse generation, passively mode-locked fiber lasers have many applications in industrial purposes and basic researches, such as optical communication, laser surgery, laser processing, seed sources and etc. [6-10] Up to now, various methods have been used to achieve passive mode locking in a fiber laser, e.g., nonlinear polarization evolution (NPE), nonlinear optical loop mirror (NOLM). In the developing process of fiber lasers, various types of pulses with different generation mechanisms have been investigated, e.g., the traditional soliton, multi-solitons, noise-like pulse (NLP), self-similar pulse, and dissipative soliton [11-15]. Achieving mode-locked fiber lasers in NLP regime has attracted much interest due to their higher energy and wider pulse width [16-18]. The NLP is a wave packet consisting of many sub picosecond pulses, which is a feasible method for increasing pulse energy despite its noisy feature [19-21]. Many materials have also been used as a saturable absorber (SA) for achieving mode locking,

which possess broadband nonlinear optical properties and ultrafast response time [22-24]. Recently, 2D nanomaterial have been widely applied in the mode-locked fiber laser due to their SA characteristics and ultrafast response, such as graphene [22,25], bismuthene [26], single-wall carbon nanotubes (SWNT) [27-30], topological insulators (TIs) [24], transition metal dichalcogenides (TMDs) [31], black phosphorus [32,33] and quantum dots (BPQDS) [34]. 2D materials have presented exceptional optical properties which expand their probable application in our daily life [5]. Up to now, bismuthene have been used in the ultrafast laser as optical switching, modulator, or SAs in 1.5-μm regimes [35]. However, bismuthene as SA applied in 1-μm ultrafast laser haven't been reported yet. Furthermore, the pulse dynamics is also needed to be investigated.

In this work, We applied bismuthene saturable absorber to Yb-doped fiber laser and obtained noise-like pulses for the first time. For integrating the bismuthene into the fiber laser, a tapered single mode fiber (SMF-28) with a loss of 35% are prepared by flame brush method. Then, the bismuthene is deposited on the tapered fiber through laser injection method. The nonlinear optics properties of bismuthene is studied by using a home-made mode-locked fiber laser, whose saturation intensity and modulation depth are about 0.4 MW/cm^2 and 3.8%, respectively. Especially, compared with traditional noise-like pulses results, the intensity ratio of coherent peak and envelope components in our cavity is of around 5:4. The generated pulses are in fact noise-like incoherent pulses made up of a complex ultrashort sub-pulse structure. This result is due to the narrow band gap of bismuthene and the dispersion and high nonlinearity of the laser cavity. The results suggest that

bismuthene could be developed as an effective nonlinear optical material for ultrafast laser and applied to related fields of ultrafast photonics in 1-μm regime.

2. Sample preparation and experimental setup

2.1. Characterizations

The electronic properties of ultrathin single-layer bismuth has been investigated by first-principles previously. In this section, we show the characterization of the prepared few-layer bismuthene. The sonochemical exfoliation method is employed to synthesize large-sized few-layer bismuthine [36-38]. Regarding the progress in experiments, we will revisit and provide a more detailed description in the following section [5]. Figure 1(a) shows a photograph of bismuthene dispersion. The microstructure and element distribution of the bismuthene were investigated by scanning electric microscopy (SEM) and energy dispersive X-ray spectroscopy (EDS). EDS analysis of bismuthene sheets randomly selected on the silicon wafer is given in Figure 1(b), which shows that atom percent of the bismuth is 100%, whereas silicon contamination might be attributed to the silicon wafer. In addition, Figure 1(c) and (d) provide the SEM images of the few-layer bismuthene with different scale. The materials which is irregular layer structure is determined by SEM. In Figure 1(e), a transmission electron microscopy (TEM) image depicts of few-layer bismuthene. Figure 1(f) gives a high-resolution TEM (HRTEM), which shows that inter-distance of the lattice fringes is 0.33 nm in accordance with the (012) interplanar distance of the rhombohedral A7 structure [35].

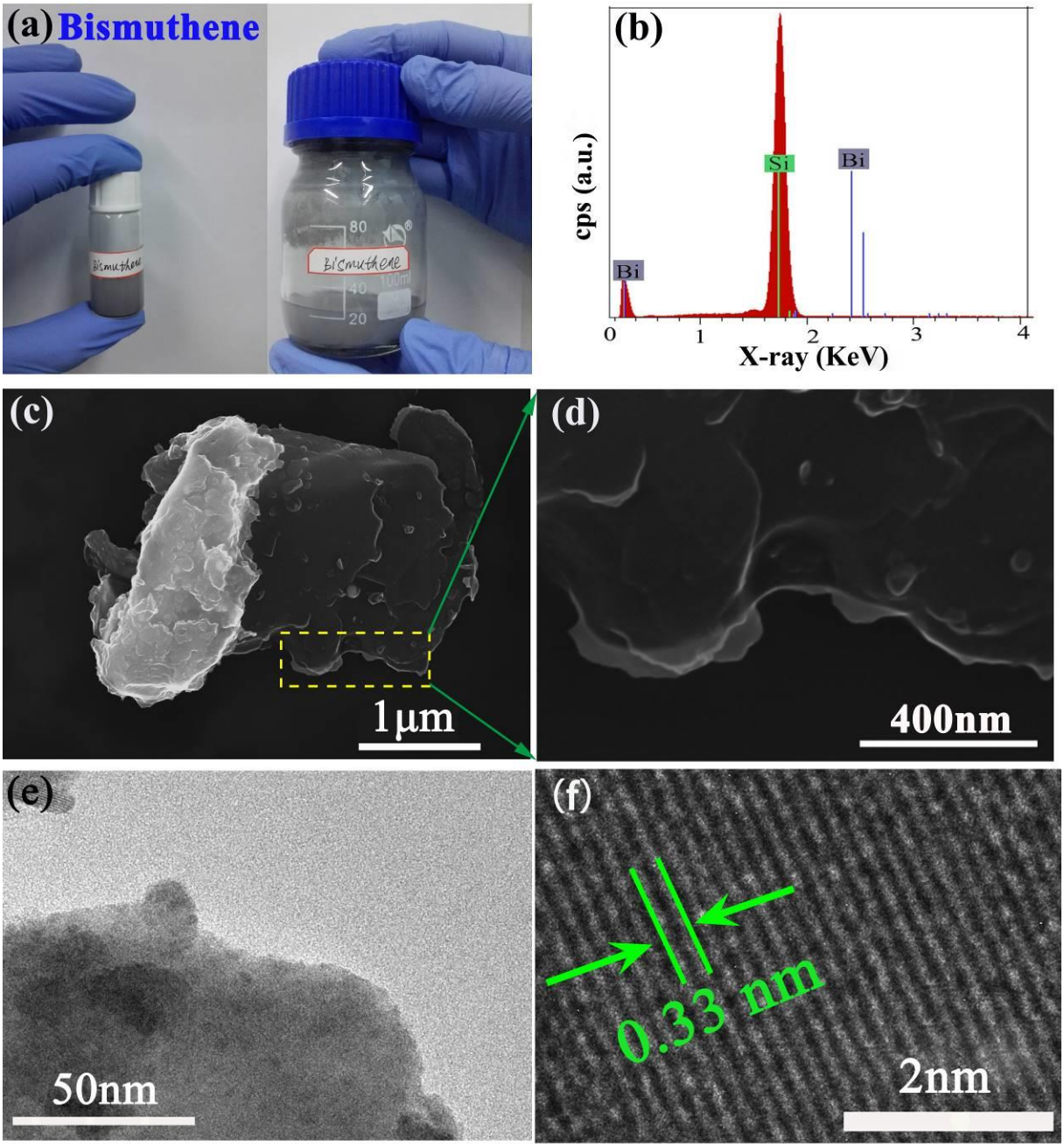

Figure 1. (a) Photograph of the bismuthene dispersion. (b) EDS analysis of bismuthene sheets randomly selected on the silicon wafer. (c) SEM image with 1 μm scale. (d) SEM image with 400 nm scale. (e) TEM image. (f) HRTEM image.

The atomic structure of bismuthene is shown in the Figure 2(a). For bismuth, only one stable form exists, which possesses a rhombohedral A7-type structure like antimony, with a natural layered structure [3,11,31]. High resolution X-ray diffraction (HRXRD) of bismuth powder is given in Figure 2(b), and its space group is confirmed to be $R\bar{3}m$ [35]. Raman spectrum of few-layer bismuthene nanoflake shown in

Figure 2(c). In earlier reports, the peaks at 69.3 cm^{-1} and 97 cm^{-1} were attributable to Raman mode and proved of the rhombohedral bismuthene structure [39]. The correlated results were almost the same. Figure 2(d) illustrates the linear absorption spectra of few-layer bismuthine measured by Lambert law in the wavelength range between 1000 and 1600 nm. Results show that the bismuthene has nonlinear absorption coefficient in wider spectrum area, which has potential applications as novel optical material [40].

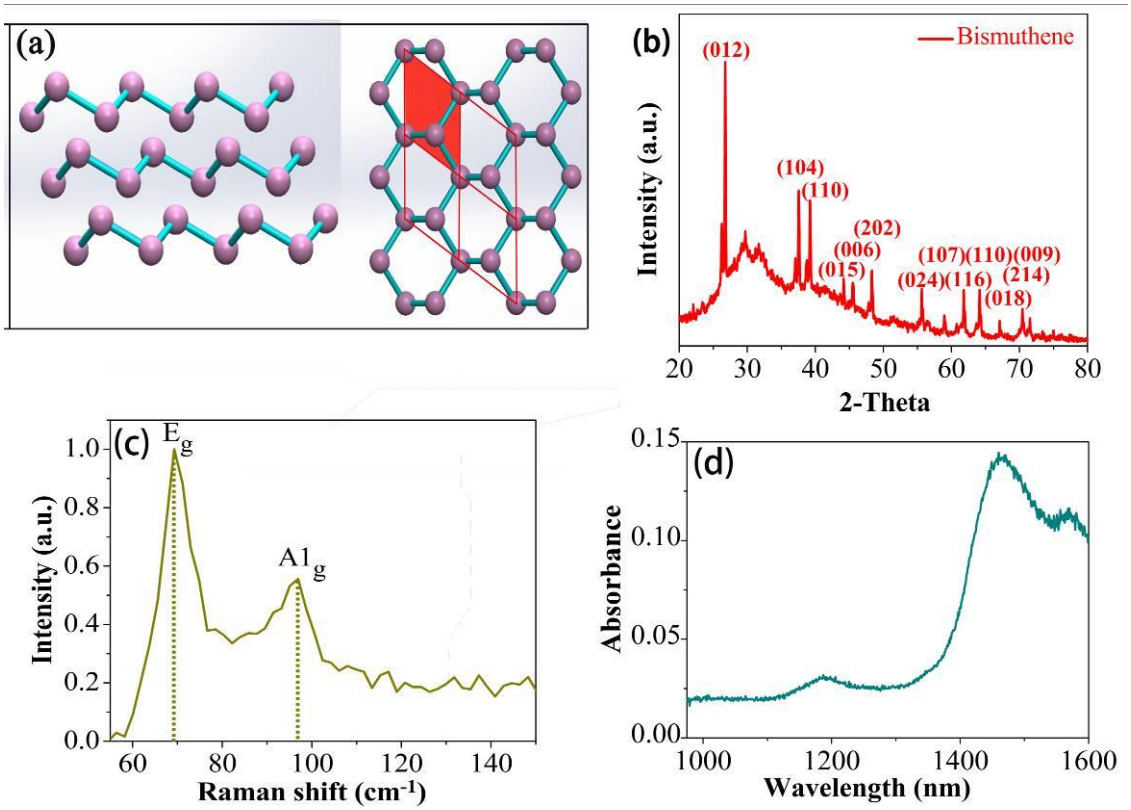

Figure 2. (a) The atomic structure of bismuthine. (b) HRXRD analysis of bismuthene. (c) Raman spectrum of the few-layer bismuthene. (d) Absorption spectrum.

2.2. Deposition of bismuthene around microfiber

In general, attaching the material onto the facet of fiber connector is the main method to prepare the SAs, which is easy to be damaged by the high energy density of ultrafast pulse. Fortunately, the issue would be avoided by utilize evanescent field interaction between fiber and material. In the next section, we will enable bismuthene as SA in the proposed fiber laser. First of all, we need to make a microfiber with a low

loss. A traditional method of preparing microfiber with single mode fiber (SMF-28) has been developed. As shown in Figure 3(a), bare part of the optical fiber is put on the alcohol light and heated. At the same time, both sides of the fiber end are stretched in two directions with a certain speed. Finally, the bare fiber is tapered with a length of 1 cm and a diameter of 13 μm. These factors are determined by the "taper" of the microfiber. The taper ratio is calculated about 1.12%. Then, we connect one end of the microfiber with the laser source and the other end to the output power meter. It can be calculated that the loss of the optical fiber is about 35%. Next, we need to deposit the bismuthene around the microfiber using a setup shown in the inset of Figure 3(a). The microfiber is connected with the 974 nm laser diode for laser deposition. The bismuthene dispersible liquid was oscillated about 40 min until the bismuthene solution was sufficiently dispersed. Then the solution was carefully added to the cone of the microfiber. The swirl and convection caused by the laser can been observed clearly under the microscope. In the meantime, we use the power meter to monitor the output power for controlling the deposition time. When the power is reduced from 36.6 mW to 17 mW, we turn off the pump immediately to stop deposition. Then, the deposited microfiber is well protected and fully dried about 12 h. After this process, about 54% power are absorbed by the bismuthene. One of the advantages of this approach is that the deposition only occurs at the boundary of the optical input, which allows us to control the deposition length. As shown in Figure 3(b), the bismuthene is deposited well around the microfiber.

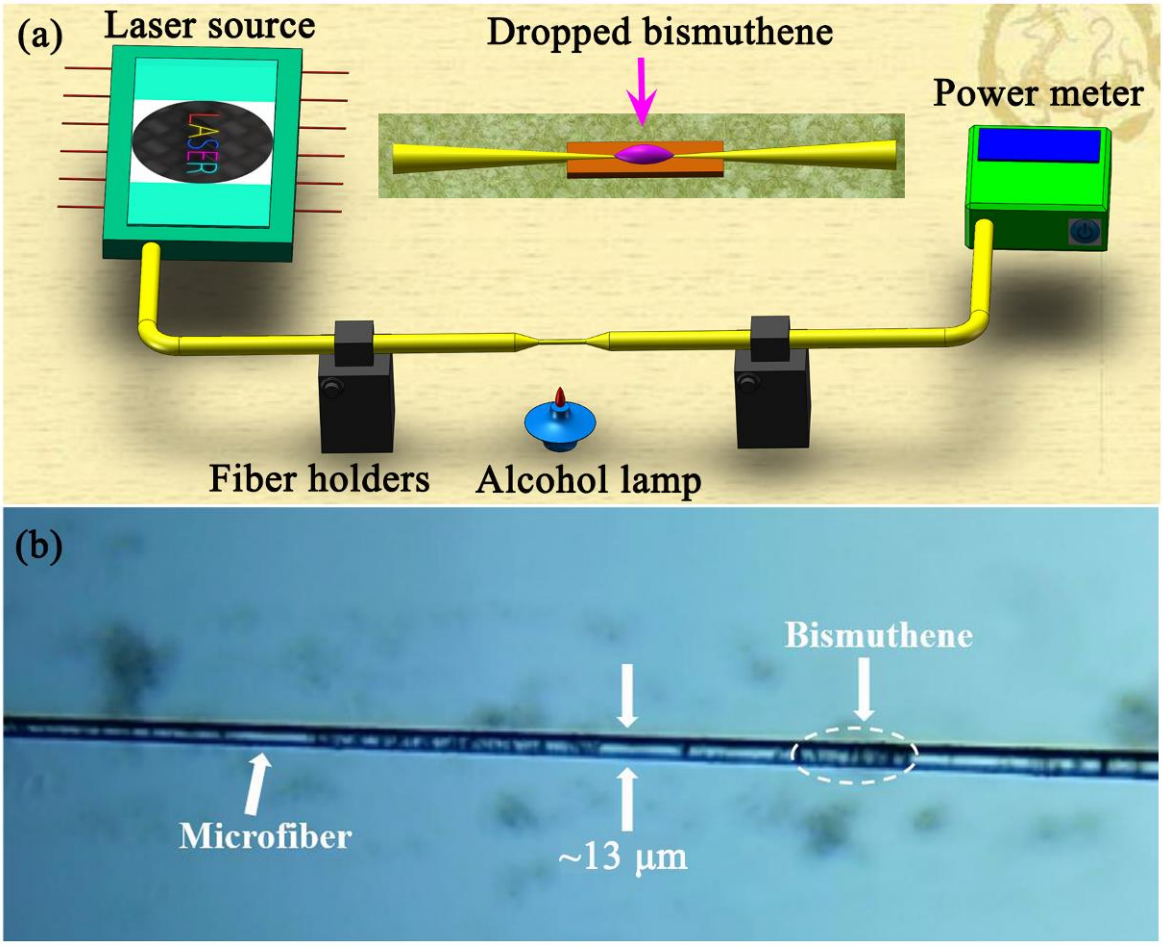

Figure 3. (a) Experimental setup for fabricating of microfiber, inset: Schematic diagram of bismuthene deposition on microfiber by injecting laser. (b) Microscope image of the prepared microfiber-based bismuthene SA.

2.3 Bismuthene microfiber SA's nonlinear characteristics

As shown in Figure 4(a), nonlinearity of bismuthene SA on self-designed testing device is tested. Test results as shown in Figure 4(b) demonstrated that bismuthene based microfiber absorber tends gradually saturation with incident light power increasing. The nonlinear transmittance of light varies from 17.5% to 21.3% and eventually reaches saturation. The calculation results show that the modulation depth of the bismuthene tapered fiber is 3.8%, which is sufficient to modulate the laser and realize the output of pulse light.

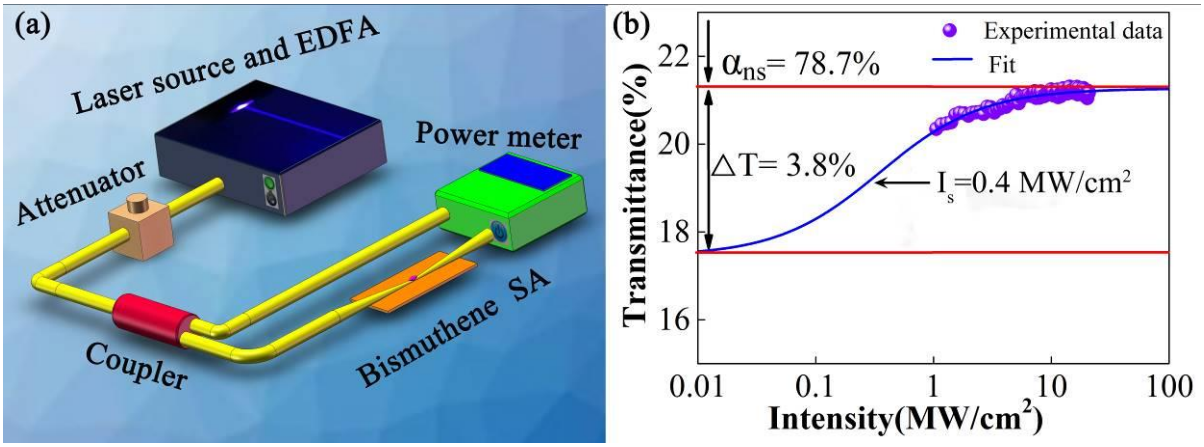

Figure 4. (a) Detector system for the nonlinear absorbance of microfiber-based bismuthene SA. (b) Nonlinear transmittance and fitting curve.

2.4 Experimental setup

As shown in Figure (5), the cavity length of fiber laser is 92 cm. The 980 nm laser diode is used to provide pump. The fiber used in our cavity is HI-1060 single mode fiber. Among them, 1-m-long ytterbium-doped (YDF, CorActive YB401) fiber as the plus medium is used in the experiments with absorption coefficient of 150 dB/m at 915 nm. There is also a polarization independent isolator in the fiber resonator and the 980/1064 wavelength division multiplexer. The polarization independent isolator is used to guarantee the laser unidirectional in resonant cavity. The SA is regarded as the nonlinear medium and the model of the optic system because its characteristic that light transmittance of SA actually increases with pulse strength. The optical pulse has some natural features as follows: low edge strength and high center strength. As soon as the optical pulse passes the SA，it will be narrowed to achieve mode-locking. The polarization controller is used to change the polarization state of the optical pulse transmission in the cavity. The laser couple in a fiber coupler with a coupling ratio 50.3:49.7, 50.3% of the pulse remain in the laser cavity, 49.7% of the pulse as output goes through a photoelectric detector (Thorlabs DET01CFC). Then, the cavity produce laser and can be connected directly from the instrument's output to the oscilloscope (Rigol DS6104) and optical spectrum analyzer (Anritsu MS9710C) to

realize rapid monitoring and measurement of the laser pulses in real-time. Quality of the mode locking are observed by a radio frequency (RF) spectrum analyzer (Rohde & Schwarz FSC6). Moreover, the pulse duration was measured by using an autocorrelator (Femtochrome FR-103XL) with the resolution of 5 fs.

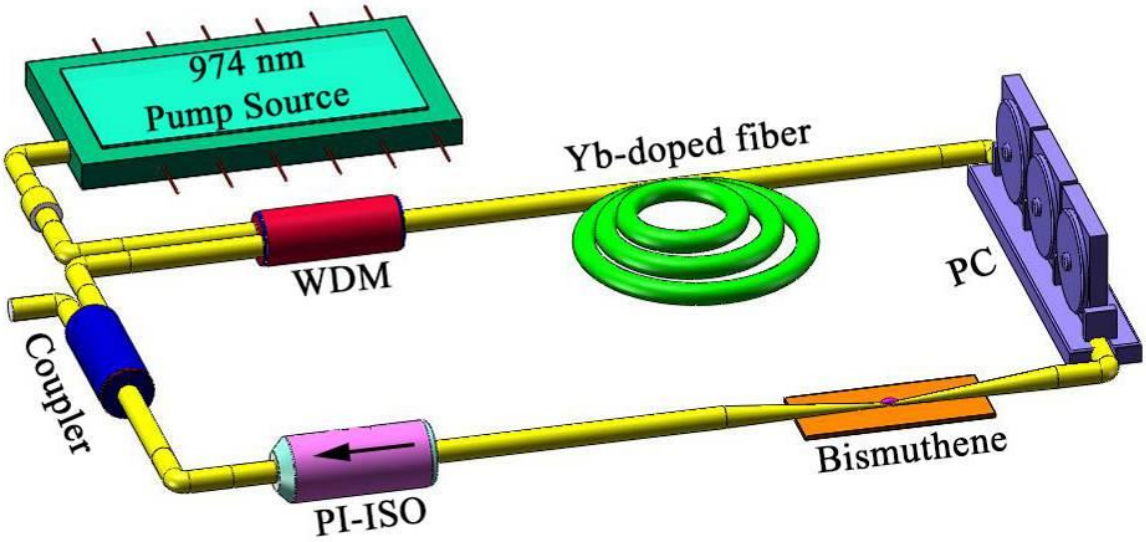

Figure 5. Schematic of mode-locked fiber laser with a microfiber-based bismuthene SA.

3. Experimental result and discussion

In the experiment, we required only few drops of the bismuthene solution. Although the amount of used bismuthenes on the surface of the microfiber is quite few, the layer-structure of bismuthene and the evanescent field is effectively coupled with each other. Self-initiated threshold of the mode-locking is 266.9 mW, and corresponding pump current is 460 mA. The spectrum is shown in Figure 6(a), from which it can be concluded that the spectrum belongs to the partially coherent pulses. The center wavelength of the spectrum and the 3-dB spectrum width is 1035.8 nm and 3.4 nm, respectively. The pulse train is shown in Figure 6(b), the time of the two pulses for the interval is 46 ns, corresponding to the period. As shown in Figure 6(c), the signal-to-noise ratio is 29.6 dB within the frequency window of 25 MHz. As shown

in Figure 6(d), the repetition frequency of the fiber laser is 21.74 MHz. As shown in Figure 6(e), the autocorrelation function of pulse contained the coherent peak (around 1.55 ps) and envelope (around 54.19 ps) components when the pump power is 266.9 mW. It can be seen from Figure 6(f) that the slope efficiency of laser is 1.71% with a linear fitting.

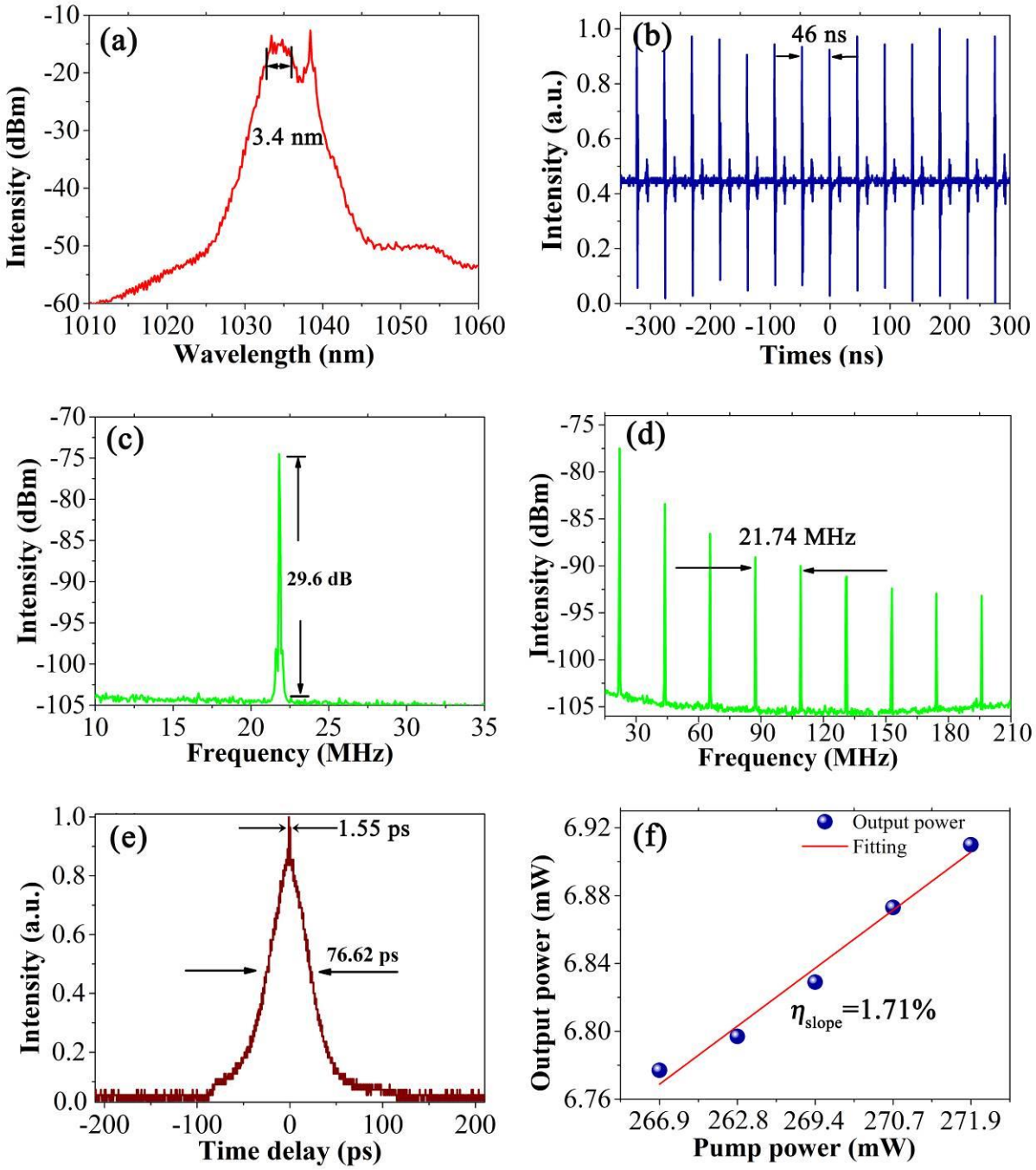

Figure 6. (a) Typical spectrum of the noise-like pulse with center wavelength of 1035.8 nm. (b) Pulse train with 46 ns period. (c) Signal-to-noise ratio is about 29.6 dB. (d) RF spectra of the pulse with 21.74 MHz repetition rate. (e) autocorrelation trace of

Partially coherent pulse generation. (f) The output power versus the pump power and the fitting slope curve.

As shown in Figure 7(a), the spectrum changes with the increase of pump power. Figure 7(c) is pulse trains with the changing of pump power. Figure 7(b) is the autocorrelation trace evolution diagram. This kind of noise pulse wave packet has a low phase coherence and random spectral fluctuation. The time domain distribution of the pulse indicated that the pulse includes a large number of phase, pulse width, and with the random peak energy. The evolution of pulse width with changing pump power is shown in Figure 7(d).

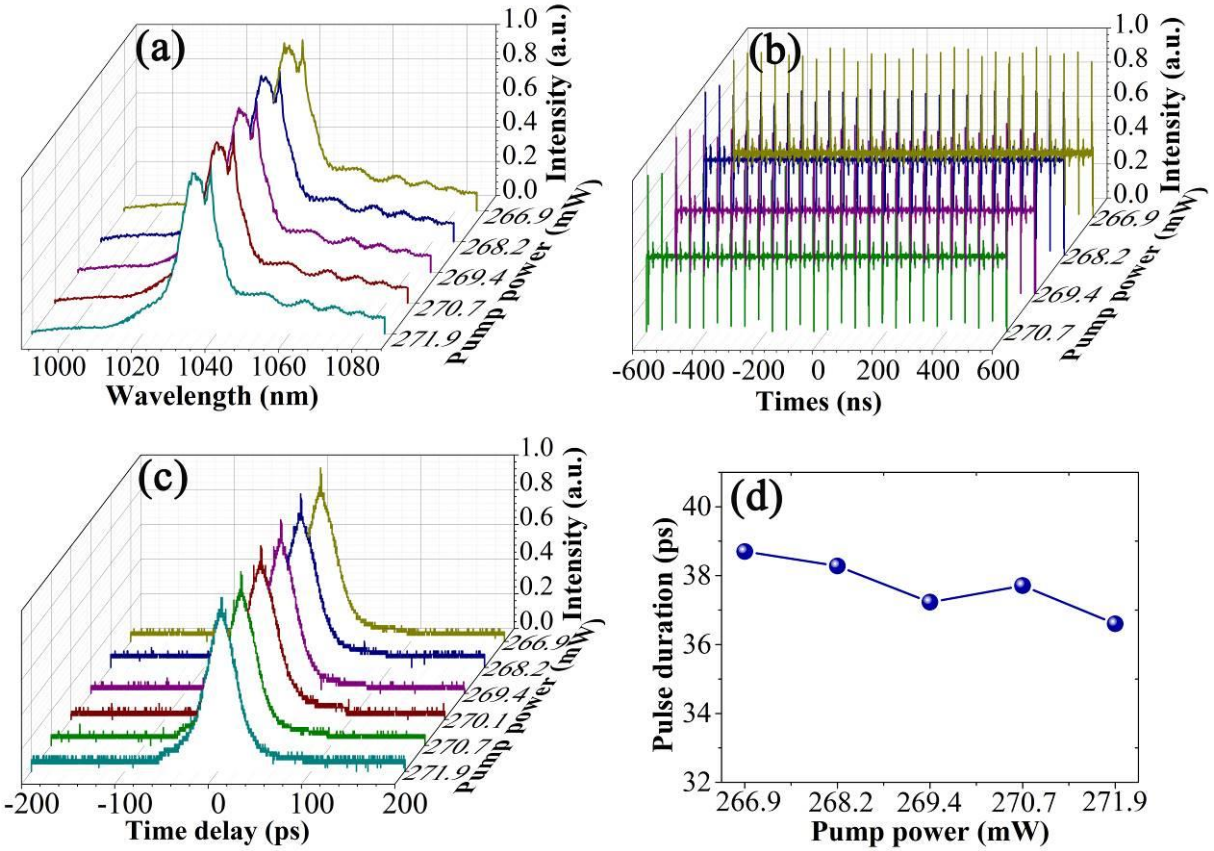

Figure 7. (a) The spectral evolution versus the pump power. (b) The pulse train evolution versus the pump power. (c) The time delay evolution versus the pump power. (d) Corresponding pulse-width evolution.

By using the self-correlation method, the width of the pedestal and the peak of the autocorrelation curve reflects the average pulse width of the class noise pulse wave packet width and the ultrashort subpulses, respectively. The pulse envelope is not split even though increasing pump power, which confirms to the characteristic of

noise-like pulse. Because of this, the noise-like pulses can be easily obtained the large pulse energy [41, 42]. In addition, the intensity ratio of the coherent peak to the envelope is 5:4 that is larger than 2:1. As all to know, conventional noise like pulses have the fixed ration with 2:1, which shows that the average intensity of the pluses is almost equal with each other. This special kind of noise-like pulses have different intensity ratio for each subpulse. We anticipate that the intensity distribution of the subpulses fits well with the Guass Distributions. So, the noise like pulse is quite unique generated in bismuthene-based Yb-doped fiber ring laser.

4. Conclusions

In this article, the Yb-doped NLP mode-locked fiber laser based on bismuthene functioned with evanescent field interaction has been demonstrated for the first time. The SA property of the bismuthene is experimentally illustrated, which saturation intensity and modulation depth of microfiber-based bismuthene SA are about 0.4 MW/cm^2 and 3.8%, respectively. A typical NLP has been obtained in fiber laser, which operates at 1035.8 nm and the autocorrelation function of pulse contains the short (around 1.55 ps) and long (around 54.19 ps) components at 21.74 MHz repetition rate. Additionally, the laser output has the bandwidth of 3.4 nm. The self-initiated threshold of mode locking is 194.1 mW, corresponding pump power is 266.9 mW. The repetition rate and signal-to-noise ratio of the output pulse for 21.74 MHz and 29.6 dB, respectively. The microfiber is used as a SA in a fiber ring laser and provided passive components for mode-locking. We believe our nonlinear optical components based on bismuthene will help the development of ultra-fast photonic devices in many fields.

Acknowledgements

This research was supported by the National Natural Science Foundation of China (grant number 61605106); Open Research Fund of State Key Laboratory of Transient Optics and Photonics, Chinese Academy of Sciences (number SKLST201401, SKLST201809); Open Research Fund of State Key Laboratory of Pulsed Power Laser Technology, Electronic Engineering Institute (No. SKL2017KF02); Open Fund of State Key Laboratory of Information Photonics and Optical Communications (Beijing University of Posts and Telecommunications), P. R. China (IPOC2017B012); Starting Grants of Shaanxi Normal University (grant number 1112010209, 1110010717); Fundamental Research Funds for the Central Universities (GK201802006, 2018CSLY005);

References

1. Yang, Q. Q.; Liu, R. T.; Huang, C.; Huang, Y. F.; Gao, L. F.; Sun, B.; Huang, Z. P.; Zhang, L.; Hu, C. X.; Zhang, Z. Q.; Sun, C. L.; Wang, Q.; Tang, Y. L.; Zhang, H. L. *Nanoscale,* **2018,** *10*, 21106-21115. DOI: 10.1039/C8NR06797J

2. Zhao, G. K.; Lin, W.; Chen, H. J.; Lv, Y. K.; Tan, X. M.; Yang, Z. M.; Mashinsky. V. M.; Krylov, A.; Luo, A. P.; Cui, H.; Luo, Z. C.; Xu, W. C.; Dianov, E. M. *Optics Express*, **2017,** *25,* 20923-20931. DOI: 10.1364/OE.25.020923

3. Wang, Q. H.; Kalantar, Z.; Kourosh, Kis, A.; Coleman, J. N.; Strano, M. S. *Nature Nanotechnology,* **2012,** *7*, 699-712. DOI: 10.1038/nnano.2012.193

4. Jiang, X. T.; Liu, S. X.; Liang, W. Y.; Luo, S. J.; He, Z. L.; Ge, Y. Q.; Wang, H. D.; Cao, R.; Zhang, F.; Wen, Q.; Li, J. Q.; Bao, Q. L.; Fan, D. Y.; Zhang, H. *Laser. Photonics. Rev.* **2018**, *12* 1700229. DOI: 10.1002/lpor.201870013

5. Zhang, S. L.; Yan, Z.; Li, Y. F.; Chen, Z. F.; Zeng, H. B. *Angew. Chem.* **2015,** *54,* 3115-3158. DOI: 10.1002/ange.201411246

6. Kamal, C.; Ezawa, M. *Phys. Rev. B.* **2014,** *91* 849-855. DOI:

10.1103/PhysRevB.91.085423

7. Zhang, Y.; Li, X. H.; Qyyum, A.; Feng, T. C.; Guo, P. L.; Jiang, J.; Zheng, H. R. *Particle & Particle Systems Characterization*, **2018,** *35,* 1800341. DOI: 10.1002/ppsc.201800341

8. Guo, Q. S.; Pospischil, A.; Bhuiyan, M.; Jiang, H.; Tian, H.; Farmer, D.; Deng, B. C.; Li, C.; Han, S. J.; Wang, H.; Xia, Q. F.; Ma, T. P.; Mueller, T.; Xia, F. N. *Nano Lett.* **2016,** *16,* 4648-4655. DOI: 10.1021/acs.nanolett.6b01977

9. Wang, X. D.; Luo, Z. C.; Liu, M.; Tang, R.; Luo, A. P.; Xu, W. C. *Laser Physics Letters,* **2016,** *13*, 045101. DOI: 10.1088/1612-2011/13/4/045101

10. Guo, Y. X.; Li, X. H.; Guo, P. L.; Zheng, H. R. *Optics Express*, **2018,** *26,* 9893-9900. DOI: 10.1364/OE.26.009893

11. Sun, Z. P.; Hasan, T.; Torrisi, F.; Popa, D.; Privitera, G.; Wang, F. Q.; Bonaccorso, F.; Basko, D. M.; Ferrari, A. C. *Acs Nano,* **2010,** *4*, 803-810. DOI: 10.1021/nn901703e

12. Zhang, S. L.; Xie, M. Q.; Li, F. Y.; Yan, Z.; Li, Y. F.; Kan, E. J.; Liu, W.; Chen, Z. F. Zeng, H. B. *Angew. Chem.* **2016,** *55,* 1666-1669. DOI: 10.1002/ange.201507568

13. Li, X. H.; Wu, K.; Sun, Z. P.; Meng, B.; Wang, Y. G.; Wang, Y. S.; Yu, X. C.; Yu, X.; Zhang, Y.; Shum, P. P.; Wang, Q. J. *Sci Rep.* **2016,** *6,* 25266. DOI: 10.1038/srep25266

14. Ma, Z. J,; Zhang, H.; Hu, Z. L.; Gan, J. L.; Yang, C. S.; Luo, Z. C.; Qiao, T.; Peng, M. Y.; Dong, G. P.; Yang, Z. M.; Frank W. W.; Qiu, J. R. *Journal of Materials Chemistry C*, **2018,** *6,* 1126-1135. DOI: 10.1039/C7TC03711B

15. Wang, X. D.; Luo, A. P.; Luo, Z. C.; Liu, M.; Zou, F.; Zhu, Y. F.; Xue, J. P.; Xu, W. C. *Laser Physics,* **2017,** *27,* 115102. DOI: 10.1088/1555-6611/aa8853

16. Lin, S. J.; Yu, J. G.; Li, W. Y. *Laser Physics,* **2019,** *29*, 025106. DOI: 10.1364/OL.42.004517

17. Jiang, G. B.; Chen, Y.; Wang, L. L.; Hu, F. R.; Zhu, P. D. *Journal of Optics*, **2019,** *21*, 015502. DOI: 10.1088/2040-8986/aaf2b2

18. Tang, D. Y.; Zhao, L. M.; Zhao, B. *Optics Express,* **2005,** *13,* 2289-2294. DOI: 10.1364/OPEX.13.002289

19. Zhao, L. M.; Tang, D. Y.; Wu, J.; Fu, X. Q.; Wen, S. C. *Optics Express,* **2007,** *15* 2145-2150. DOI: 10.1364/OE.15.002145

20. Li, X. H.; Yu, X. C.; Sun, Z. P.; Yan, Z. Y.; Sun, B.; Cheng, Y.; Yu, X.; Zhang Y.; Wang, Q. J. *Sci Rep.* **2015,** *5,* 16624. DOI: 10.1038/srep16624

21. Luo, Z. C.; Liu, M.; Liu, H.; Zheng, X. W.; Luo, A. P.; Zhao, C. J.; Zhang, H.; Wen, S. C.; Xu, W. C. *Opt. Lett.* **2013,** *38,* 5212-5215. DOI: 10.1364/OL.38.005212

22. Ersan, F.; Aktürk, E.; Ciraci, S. *Phys. Rev B.* **2016,** *94,* 245417. DOI: 10.1103/PhysRevB.94.245417

23. Ge, Y.; Zhu, Z.; Xu, Y.; Chen, Y.; Chen, S.; Liang, Z.; Song, Y.; Zou, Y.; Zeng, H.; Xu, S.; Zhang, H.; Fan, D. *Adv. Opt. Mater.* **2018,** *6,* 1870014. DOI: 10.1002/adom.201870014

24. Wang, W. Q.; Yue, W. J.; Liu, Z. Z.; Shi, T. C.; Du, J.; Leng, Y. X.; Wei, R. F.; Ye, Y. T.; Liu, C.; Liu X. F.; Qiu, J. R. *Adv. Optical Mater.* **2018,** *6*, 1700948. DOI: 10.1002/adom.201700948

25. Li, X. H.; Tang, Y. L.; Yan, Z. Y.; Wang, Y.; Meng, B.; Liang, G. Z.; Sun, H. D.; Yu, X.; Zhang, Y.; Cheng X. P.; Wang, Q. J. *IEEE Journal of Selected Topics in Quantum Electronics*, **2014,** *20,* 441-447. DOI: 10.1109/JSTQE.2014.2312952

26. Chai, T.; Li, X. H.; Feng, T. C.; Guo, P. L.; Song, Y. F.; Chen, Y. X.; Zhang, H. *Nanoscale,* **2018,** *10,* 17617-17622. DOI: 10.1039/C8NR03068E

27. Li, X. H.; Wang, Y. G.; Wang, Y. S.; Zhao, W.; Yu, X. C.; Sun, Z. P.; Cheng, X. P.; Yu, X.; Zhang, Y.; Wang, Q. J. *Optics Express*, **2014,** *22*, 17227-17235. DOI: 10.1364/OE.22.017227

28. Chernysheva, M.; Mou, C. B.; Arif, R.; AlAraimi, M.; Rummeli, M.; Turitsyn, S.; Rozhin, A. *Scientific Reports*, **2016,** *6,* 24220. DOI: 10.1038/srep24220

29. Wu, K.; Li, X. H.; Wang, Y. G.; Wang, Q. J.; Ping, S. P.; Chen, J. P.; *Optics Express*, **2015,** *23*, 501-511. DOI: 10.1364/OE.23.000501

30. Lee, J. H.; Lee, J. H. *Chinese Physics B.* **2018,** *27*, 1674-1056. DOI: 10.1088/1674-1056/27/9/094219

31. Kadir, N. A. A.; Smail, E. I. I.; Latiff, A. A. *Chinese Physics Letters,* **2017,** *34*, 48-51. DOI: 10.1088/0256-307X/34/1/014202

32. Wang, J. L.; Xing, Y. P.; Chen, L.; Li, S.; Jia, H. T.; Zhu, J. F.; Wei, Z. Y. *Journal of Lightwave Technology,* **2018,** *36*, 2010-2016. DOI: 10.1109/JLT.2018.2800910

33. Li, W. L.; Chen, G. W.; Wang, G. M.; Zeng C.; Zhao, W. *Laser Physics Letters,* **2018,** *15*, 125102. DOI: 10.1088/1612-202X/aae786

34. Zhang, S. L.; Guo, S. Y.; Chen, Z. F.; Wang, Y. L.; Gao, H. J.; Gomez-Herrero, J.; Ares, P.; Zamora, F.; Zhu, Z.; Zeng, H. B. *Chemical Society Reviews,* **2018,** *47,* 982-1021. DOI: 10.1039/C7CS00125H

35. Lu, L.; Liang, Z. M.; Wu, L. M.; Chen, Y. X.; Song, Y. F.; Dhanabalan, S. C.; Ponraj, J. S.; Dong, B. Q.; Xiang, Y. J.; Xing, F.; Fan, D. Y.; Zhang, H. *Laser & Photonics Reviews,* **2018,** *12*, 1700221. DOI: 10.1002/lpor.201700221

36. Chen, R. B.; Jang, D. J.; Lin, M. C.; Lin, M. F. *Optics Letters*, **2018,** *43* , 6089-6092. DOI: 10.1364/OL.43.006089

37. Mario, L. Y.; Darmawan, S.; Chin, M. K. *Optics Express*, **2006,** *14,* 12770-81. DOI: 10.1364/OE.14.012770

38. Lu, L.; Wang, W. H.; Wu, L. M.; Jiang, X. T.; Xiang, Y. J.; Li, J. Q.; Fan, D. Y.; Zhang, H. *Acs Photonics,* **2017,** *4*, 2852-2861. DOI: 10.1021/acsphotonics.7b00849

39. Wang, L.; Li, X. H.; Luo, W. F.; Feng, T. C.; Zhang, Y; Guo, P. L.; Ge, Y. Q. *Nanotechnology*, **2018,** *30,* 025204. DOI: 10.1088/1361-6528/aae8c1

40. Kobtsev, S.; Kukarin, S.; Smirnov, S.; Turitsyn, S.; Latkin, A. *Optics Express*, **2009,** *17*, 20707-13. DOI: 10.1364/OE.17.020707

41. Lin, Y. H.; Lin, S. F.; Chi, Y. C.; Wu, C. L.; Cheng, C. H.; Tseng, W. H.; He, J. H.; Wu, C. I.; Lee C. K.; Lin, G. R. *Acs Photonics*, **2015,** *2*, 481-490. DOI: 10.1021/acsphotonics.5b00031

42. Lv, Z. G.; Yang, Z.; Song, D. D.; Li, F.; Yang, X. J.; Yang, Y.; Wang, Y. S.; Li, Q. L.; Zhao, W. *Applied Physics Express,* 2019, *12,* 022004. DOI: 10.7567/1882-0786/aaf417